



CHORUS

This is the accepted manuscript made available via CHORUS. The article has been published as:

Adsorbed water-molecule hexagons with unexpected rotations in islands on Ru(0001) and Pd(111)

Sabine Maier, Ingeborg Stass, Toshiyuki Mitsui, Peter J. Feibelman, Konrad Thürmer, and Miquel Salmeron

Phys. Rev. B **85**, 155434 — Published 16 April 2012

DOI: [10.1103/PhysRevB.85.155434](https://doi.org/10.1103/PhysRevB.85.155434)

Water-molecule arrangements on Ru(0001) and Pd(111) - a new twist

Sabine Maier,^{1,*} Ingeborg Stass,^{1,2} Toshiyuki Mitsui,^{1,†} Peter
J. Feibelman,³ Konrad Thürmer,⁴ and Miquel Salmeron^{1,5,‡}

¹*Lawrence Berkeley National Laboratory, Berkeley, CA 94720*

²*Institut für Experimentalphysik, Freie Universität Berlin, Arnimallee 14, 14195 Berlin, Germany*

³*Sandia National Laboratories, Albuquerque, NM 87185-1415*

⁴*Sandia National Laboratories, Livermore, CA 94550*

⁵*Materials Science and Engineering Department, University of California, Berkeley, CA 94720*

(Dated: March 20, 2012)

High-resolution Scanning Tunneling Microscopy (STM) reveals that the first layer of water on Ru(0001) and also on Pd(111) consists of hexagonal molecular domains of two types, rotated by 30° relative to one another. Pentagon and heptagon clusters bridge the two types of hexagons. One of the orientations is in registry with the substrate. Its molecules lie flat and their O atoms form strong bonds to the metal atoms lying directly below. In the other domain the molecules have dangling H-bonds. They are weakly bound to the substrate and lie correspondingly higher. This bonding motif, though non-periodic, is of similar nature to the periodic wetting structure recently reported on Pt(111), and very different from the conventional "ice-like" bilayer. First-principles Density Functional Theory (DFT) simulations of the STM images support these conclusions.

PACS numbers: 68.55.-a 68.37.Ef 68.43.Hn

I. INTRODUCTION

The first wetting layer on a solid is the template for ice nucleation, governs aqueous surface chemistry, and embodies the boundary condition for water transport along its surface. Accordingly, the arrangement and energetics of wetting layers is important, governing the little understood physics of the "no-slip" boundary condition commonly imposed on Navier-Stokes flows in confined spaces,¹ the identity of the most efficient seeds for raindrop formation,² and electrode effects on the rates and selectivity of electrochemical reactions³.

Water molecule arrangements in wetting layers have until very recently been studied not by acquiring molecular scale scanning probe images, but, because of their fragility, by attempting to interpret indirect evidence provided by vibration and thermal desorption spectra, and by k-space measurements like Low Energy Electron Diffraction (LEED) and Helium Atom Scattering (HAS). On close-packed hexagonal metal surfaces, including Ru(0001), HAS and LEED experiments implied that wetting layers adopt a $\sqrt{3} \times \sqrt{3}$ - R30° periodicity.⁴⁻⁷ Thus, on grounds of simplicity, and setting aside the LEED evidence that the O-atoms in the structure are coplanar⁷, wetting was attributed to the formation of an "ice-like" structure strained into registry with the metal atoms but otherwise coordinated just like the hexagonal layers that stack to form the naturally occurring ice Ih crystal.

Only years later did DFT calculations make clear that the ordered, coplanar O structure on Ru(0001) cannot be an arrangement of intact water molecules - the adsorption energy of such a structure is far too low - but a partially dissociated layer of H₂O-OH,⁸ formed upon sufficient heating or exposure to electrons. That left the nature of wetting arrangements of intact water molecules obscure. LEED, which is insensitive to H-atom positions, indicates O-atom ordering⁷, whereas broad RAIRS bands⁹, low reflectivity and broad peaks in He scattering¹⁰ imply a disordered phase. Theoretical efforts have provided hints, notably that a H-bonded honeycomb network with alternating chains of flat-lying molecules and of those with dangling H-bonds has a particularly low energy^{9,10}. However, no theoretical model can be accepted that conflicts with STM images. At submonolayer coverage, such images for water on Pd(111) and on Ru(0001) show narrow water clusters of well-defined maximal width. This width appears to result of topological constraints on the number of flat-lying water molecules that can bind strongly to the underlying metal via the lone-pair orbitals of the O atoms, while connecting to each other by H-bonds^{11,12}. To extend an island's width to more than one hexagonal cluster, as in the "rosette" shown in Fig. 1(b), a certain number of dangling bond molecules must continue the structure, even though they bind weakly to the surface.

Nie et al.'s recent examination of water on Pt(111)¹³ has provided a new way to think about wetting layer structures. Their STM data showed that the first water layer on Pt(111) has two levels, and that its periodicity reflects an ordered arrangement of patches of low-lying water molecules. In the ice-like model, the water layer on Pt(111) should show no height variations beyond those imposed by the alternation of flat-lying water molecules, and those having a dangling H-bond. Nie et al.'s analysis, however, implied that the low-lying molecules anchor the water layer to the metal, and that this is only possible if these low patches are surrounded by higher-lying "ribbons" of water molecules, weakly bonded to the metal and arranged in hexagons rotated 30° relative to the primitive directions of the Pt crystal surface.

Here we present new high resolution images showing that similar - though non-periodic - arrangements of low-lying clusters in registry with the substrate and high-lying clusters rotated 30° occur on the Pd(111) and Ru(0001) surfaces. We still do not understand why kinetic barriers are low enough on Pt(111) to facilitate ordering but not on Pd(111) or Ru(0001). Nonetheless, by means of STM imaging, we are on the way to develop a common framework for understanding how water binds to close-packed precious metal substrates.

II. METHODS

The experimental results reported here were obtained using scanning tunneling microscopy in two separate instruments.^{14,15} A clean ruthenium surface was prepared by annealing cycles in oxygen between 800 K and 1800 K and a clean palladium surface by sputtering at 1000 K with subsequent flashing to 1100 K, respectively. Imaging was performed at temperatures around 7-80 K (Ru) and 80-100 K (Pd). These cleaning procedures produced well-ordered surfaces with less than 1 % surface impurities including subsurface impurities. H₂O (Sigma Aldrich, deuterium depleted, 99.99995 %) and D₂O were purified by pump and thaw cycles prior to introduction into the UHV chamber via a leak valve and a dosing tube pointing toward the metal surface.

The most stable adsorption structure of water on Ru(0001) is a partially dissociated hydrogen-bonded network of H₂O and OH, rather than a layer of intact water.⁸ Dissociation however requires overcoming an activation barrier of

0.5 eV or more, which can be achieved by heating the sample above 140 K. For Pd(111), XPS measurements revealed no signs of thermally induced partial dissociation when water was adsorbed on the clean surface, at 145 K.¹⁶ In our experiments we deposited monolayer amounts of water mostly at low temperature, followed by heating between 110 and 140 K, on Ru(0001), and to 80-100 K on Pd(111). Depositing water directly at 140 K for Ru and at 80-100 K for Pd yields the same structures as does dosing at low temperatures followed by an annealing cycle to same temperatures. These temperatures are low enough to rule out dissociation of water and high enough to promote its diffusion. Intact water on Ru(0001) can also be converted to a mixed H₂O-OH phase through excitation by the tunneling electrons when their energy is 0.5 eV or higher above the Fermi level.^{17,18} Thus, to avoid any tip-induced dissociation, all STM images shown in this paper were acquired with bias voltages well below this value.

We performed binding energy calculations with the VASP DFT code,^{19,20} representing exchange-correlation effects in the Perdew-Burke-Ernzerhof (PBE) implementation of the Generalized Gradient Approximation,²¹ and treating electron-nucleus interactions in the projector augmented wave (PAW) approximation.^{22,23} We modeled the Ru(0001) substrate as a 3-layer slab, with water adsorbed on its upper surface only. The atoms of the lower layer were fixed in theoretical bulk Ru positions (corresponding to an in-plane lattice constant $a_{PBE} = 2.725 \text{ \AA}$), and all other atom positions were free to relax. To prevent water clusters from interacting with each other, we placed them in a $2\sqrt{37} \times 2\sqrt{37}$ surface supercell, such that the nearest O atoms in two different clusters were no closer than 14.4 Å. We sampled the surface Brillouin zone at the gamma-bar point only, and, for high accuracy, used a 700 eV plane-wave basis cutoff. We used Methfessel-Paxton Fermi-level smearing²⁴ (width=0.2 eV) to accelerate electronic relaxation, and implemented Neugebauer-Scheffler corrections²⁵ to cancel the unphysical fields associated with the periodic repeats normal to the asymmetric model slab. Geometry relaxation was deemed converged when forces on all but the lower Ru layer atoms were smaller than 0.045 eV/Å in magnitude.

III. RESULTS AND DISCUSSION

At low coverage water forms honeycomb domains in registry with the substrate. As described in previous work^{11,12} these domains are of limited size to minimize the number of non-flat molecules. At higher coverage new domains of hexagonal clusters are formed on both Ru(0001) and Pd(111) which, as shown in the STM images of Fig. 2, have different heights. The high domain (brighter hexagons) appears 40-50 pm above the initial low domain (darker), where the molecules are located 80-110 pm above the Ru surface. A few individual bright spots (200-220 pm above the metal surface) preferentially decorating the edges of the high-lying water domains correspond to molecules in the second layer. The alternation between high and low-lying domains does not manifest long-range order, in contrast with the Pt(111) surface, on which water arranges into periodic $\sqrt{37} \times \sqrt{37}$ -R25.3° and $\sqrt{39} \times \sqrt{39}$ -R16.1° supercells.^{13,26,27} Moreover, the hexagons in the high-lying domains are rotated 30° with respect to those in the low lying domains, and with the hexagonal lattice of the metal surface. This is shown more clearly in figure 3. The transition between bright and dark domains is mediated by pentagonal and heptagonal ring structures, as shown in Fig. 4. We found these two-domain structures at temperatures ranging from 80 K (Fig. 2(b) and Fig. 3(b)), a temperature at which multilayer deposition leads to amorphous solid water²⁸, up to 140 K. That this structural motif occurs over such a wide temperature range suggests that it is energetically preferred and not merely a kinetic phenomenon.

The reason that water hexagons rotated 30° with respect to the close-packed substrate directions "should not" occur is that individual water molecules prefer to bind with their O atoms directly above metal atoms, with 0.2 to 0.3 eV higher energy according to first-principles calculations.^{17,29} In the face of this number, large compared to kT , the mystery is how inter O-atom vectors can be other than parallel to the primitive vectors of the underlying surface. The paradox is resolved by the recognition that the wetting layer segregates into regions of flat-lying molecules, whose O atoms lie atop metal atoms, forming strong bonds to them, and regions of dangling H-bond molecules, whose O atoms lie considerably higher.

At submonolayer coverage the high-lying domains tend to be located in the center of the water clusters on both Pd(111) (Fig. 5) and Ru(0001) (Fig. 3(c)). One expects the opposite if the flat hexagons of the low domain grow first^{11,12}. On the other hand, given that each domain has a limited width, the high-lying domains should be surrounded by a shell of flat molecules, thus maximizing the molecular fraction that is strongly bound. That such a configuration is indeed observed indicates that the annealing temperature after deposition was sufficiently high for the molecules to rearrange into a structure closer to equilibrium.

Numerous DFT calculations imply that dangling H-bond molecules lie relatively high, with 3.5 Å above the metal being a representative height. This is several tenths of an Å greater than typical O-metal atom bond lengths.^{8,29} This

is true whether the dangling H lies on the vacuum side of the O, or between the O and the metal. In the latter case, the molecule must lie high to accommodate the size of the underlying H atom. In the former it is because the O($2p_z$) orbital is already hybridized with the H(1s), leaving no valence electron to form a bond with the underlying metal.⁸ Thus, dangling H-bond molecules are only slightly attracted to the substrate and sense the corrugation of the surface weakly. Given that the regions of rotated hexagons are populated by such molecules, it is clear why the 30° rotation costs little binding energy.

But, is there an advantage to having regions with the unexpected azimuthal orientation? This follows from the notion that distorting a perfect honeycomb into a two-level arrangement of clusters would overly stretch the H-bonds at the boundary between the levels. Stretched bonds can be avoided, however, by inserting extra molecules. A natural way to add them without breaking bonds is to incorporate them in boundaries between clusters of differently rotated hexagons.¹³ Replacing four water molecules arranged in a "Y" by a hexagon converts a flat, hexagonally-coordinated mesh of H₂O into a two-level mesh, with hexagons of flat-lying H₂O connected by 5- and 7-fold rings of molecules, to chains of dangling-H molecules in hexagons misoriented azimuthally by 30° . Recently, water-molecule pentagons have also been observed on Cu(110).³⁰

We performed VASP structural optimizations^{19,20} followed by STM image simulations to test this scenario. The STM image in Fig. 6(a) shows an image of a cluster of water on Ru(0001) containing high-lying and low-lying hexamers rotated 30° from each other, and connected by pentagons and heptagons. Fig. 6(b) is a schematic of a corresponding structural model, which has been relaxed by DFT calculations, confirming that compact clusters of anchoring flat-lying H₂O molecules and rotated high-lying molecules bridged by heptagons and pentagons can form stably. The simulated STM image shown in Fig. 6(c) corresponding to this model is a contour plot showing the height above the Ru surface of a constant electron-density contour ($4.1 \times 10^{-6} e/\text{\AA}^3$) attributable to electrons from the Fermi level to 0.137 eV below. Qualitatively, the STM image simulation agrees well with experiment, with a height difference of roughly 90 pm between the low lying and high lying domains, as observed.

These results, and those by Nie et al.¹³, indicate that on Pt(111), Ru(0001) and Pd(111), the structure of large adsorbed clusters of intact water molecules is driven by the same physics and topological constraints. Nevertheless, rotated water structures of the first wetting layer need not be the most stable when more than one layer of water is present. A film with ice-like character will eventually form as hydrogen-bonding between layers becomes dominant over the water metal interaction.³¹⁻³³ Informed by our new understanding of the first water layer at the molecular level, the transition between one and multiple layers of water is a timely subject to revisit.

IV. CONCLUSION

In conclusion, new high resolution STM measurements supported by DFT calculations provide a consistent picture of the structure of intact wetting layers on Ru(0001) and Pd(111) surfaces. Hence after more than a decade of research the structure of intact water layers on two of the most studied model systems for water adsorption has been resolved. Knowing the structure of the interfacial water layer is the first step in understanding wetting. It will also lead to a better understanding of the reaction of water with other adsorbed molecules, with important applications in technology and many areas of science, e.g. catalysis and corrosion.

ACKNOWLEDGMENTS

The work was supported by the DOE Office of Basic Energy Sciences, Division of Materials Science and Engineering of the US DOE under Contracts No. DE-AC04-94AL85000 (SNL, theory) and DE-AC02-05CH11231 (LBNL, experiment).

-
- * Present address: Department of Physics, University of Erlangen-Nürnberg, 91058 Erlangen, Germany
† Present address: Department of Physics and Mathematics, Aoyama Gakuin University, Kanagawa, 252-5258 Japan
‡ mbsalmeron@lbl.gov
- ¹ P. Thompson and S. Troian, *Nature* **389**, 360 (1997).
 - ² V. Sadtchenko, G. E. Ewing, D. R. Nutt, and A. J. Stone, *Langmuir* **18**, 4632 (2002).
 - ³ J. S. Filhol and M. Neurock, *Angewandte Chemie International Edition* **45**, 402 (2006).
 - ⁴ P. A. Thiel and T. E. Madey, *Surface Science Reports* **7**, 211 (1987).
 - ⁵ D. L. Doering and T. E. Madey, *Surface Science* **123**, 305 (1982).
 - ⁶ T. Kondo, S. Mae, H. S. Kato, and M. Kawai, *Surface Science* **600**, 3570 (2006).
 - ⁷ G. Held and D. Menzel, *Surface Science* **316**, 92 (1994).
 - ⁸ P. J. Feibelman, *Science* **295**, 99 (2002).
 - ⁹ S. Haq, C. Clay, G. R. Darling, G. Zimbitas, and A. Hodgson, *Physical Review B* **73**, 115414 (2006).
 - ¹⁰ M. Gallagher, A. Omer, G. R. Darling, and A. Hodgson, *Faraday Discussions* **141**, 231 (2009).
 - ¹¹ J. Cerda, A. Michaelides, M. L. Bocquet, P. J. Feibelman, T. Mitsui, M. Rose, E. Fomin, and M. Salmeron, *Physical Review Letters* **93**, 116101 (2004).
 - ¹² M. Tatarikhov, D. F. Ogletree, F. Rose, T. Mitsui, E. Fomin, S. Maier, M. Rose, J. I. Cerda, and M. Salmeron, *Journal of the American Chemical Society* **131**, 18425 (2009).
 - ¹³ S. Nie, P. J. Feibelman, N. C. Bartelt, and K. Thürmer, *Physical Review Letters* **105**, 026102 (2010).
 - ¹⁴ S. Behler, M. K. Rose, J. C. Dunphy, D. F. Ogletree, M. Salmeron, and C. Chapelier, *Review of Scientific Instruments* **68**, 2479 (1997).
 - ¹⁵ T. K. Shimizu, A. Mugarza, J. I. Cerda, M. Heyde, Y. B. Qi, U. D. Schwarz, D. F. Ogletree, and M. Salmeron, *Journal of Physical Chemistry C* **112**, 7445 (2008).
 - ¹⁶ A. Shavorskiy, M. J. Gladys, and G. Held, *Phys. Chem. Chem. Phys.* **10**, 6150 (2008).
 - ¹⁷ A. Michaelides, A. Alavi, and D. A. King, *Journal of the American Chemical Society* **125**, 2746 (2003).
 - ¹⁸ M. Tatarikhov, E. Fomin, M. Salmeron, K. Andersson, H. Ogasawara, L. G. M. Pettersson, A. Nilsson, and J. I. Cerda, *The Journal of Chemical Physics* **129**, 154109 (2008).
 - ¹⁹ G. Kresse and J. Furthmüller, *Physical Review B* **54**, 11169 (1996).
 - ²⁰ G. Kresse and J. Hafner, *Physical Review B* **49**, 14251 (1994).
 - ²¹ J. Perdew, K. Burke, and M. Ernzerhof, *Physical Review Letters* **77**, 3865 (1996).
 - ²² P. Blöchl, *Physical Review B* **50**, 17953 (1994).
 - ²³ G. Kresse and D. Joubert, *Physical Review B* **59**, 1758 (1999).
 - ²⁴ M. Methfessel and A. Paxton, *Physical Review B* **40**, 3616 (1989).
 - ²⁵ J. Neugebauer and M. Scheffler, *Physical Review B* **46**, 16067 (1992).
 - ²⁶ A. L. Glebov, A. P. Graham, A. Menzel, and J. P. Toennies, *Journal of Chemical Physics* **106**, 9382 (1997).
 - ²⁷ S. Standop, A. Redinger, M. Morgenstern, T. Michely, and C. Busse, *Physical Review B* **82**, 161412 (2010).
 - ²⁸ J. M. K. Donev, Q. Yu, B. R. Long, R. K. Bollinger, and J. S. C. Fain, *The Journal of Chemical Physics* **123**, 044706 (2005).
 - ²⁹ S. Meng, E. G. Wang, and S. W. Gao, *Physical Review B* **69**, 195404 (2004), 195404.
 - ³⁰ J. Carrasco, A. Michaelides, M. Forster, S. Haq, R. Raval, and A. Hodgson, *Nat Mater* **8**, 427 (2009).
 - ³¹ G. A. Kimmel, N. G. Petrik, Z. Dohnalek, and B. D. Kay, *Physical Review Letters* **95**, 166102 (2005).
 - ³² K. Thürmer and N. C. Bartelt, *Physical Review Letters* **100**, 186101 (2008).
 - ³³ G. Zimbitas, S. Haq, and A. Hodgson, *Journal of Chemical Physics* **123**, 174701 (2005).

FIGURES

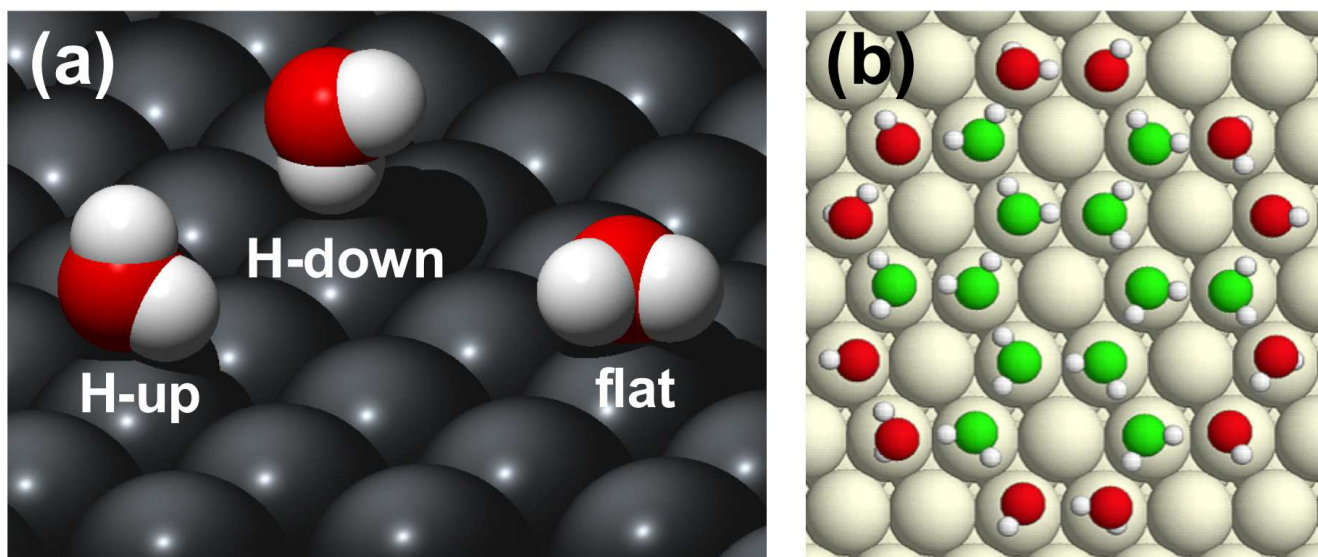


FIG. 1. (Color online) Models of water adsorption on hexagonal closed packed metal surfaces. (a) Schematic illustration of water molecules with their plane parallel (flat) and vertical to the surface, with either one H pointing up into the vacuum (H-up) or down toward the surface (H-down). (b) The cluster of flat-lying (green) molecules in the center of the cluster cannot be extended with more flat-lying molecules. Accordingly, the periphery of the rosette consists of twelve (red) dangling-H water molecules (\sim vertical), in this case with their dangling H atoms lying between their O atoms and the underlying metal.

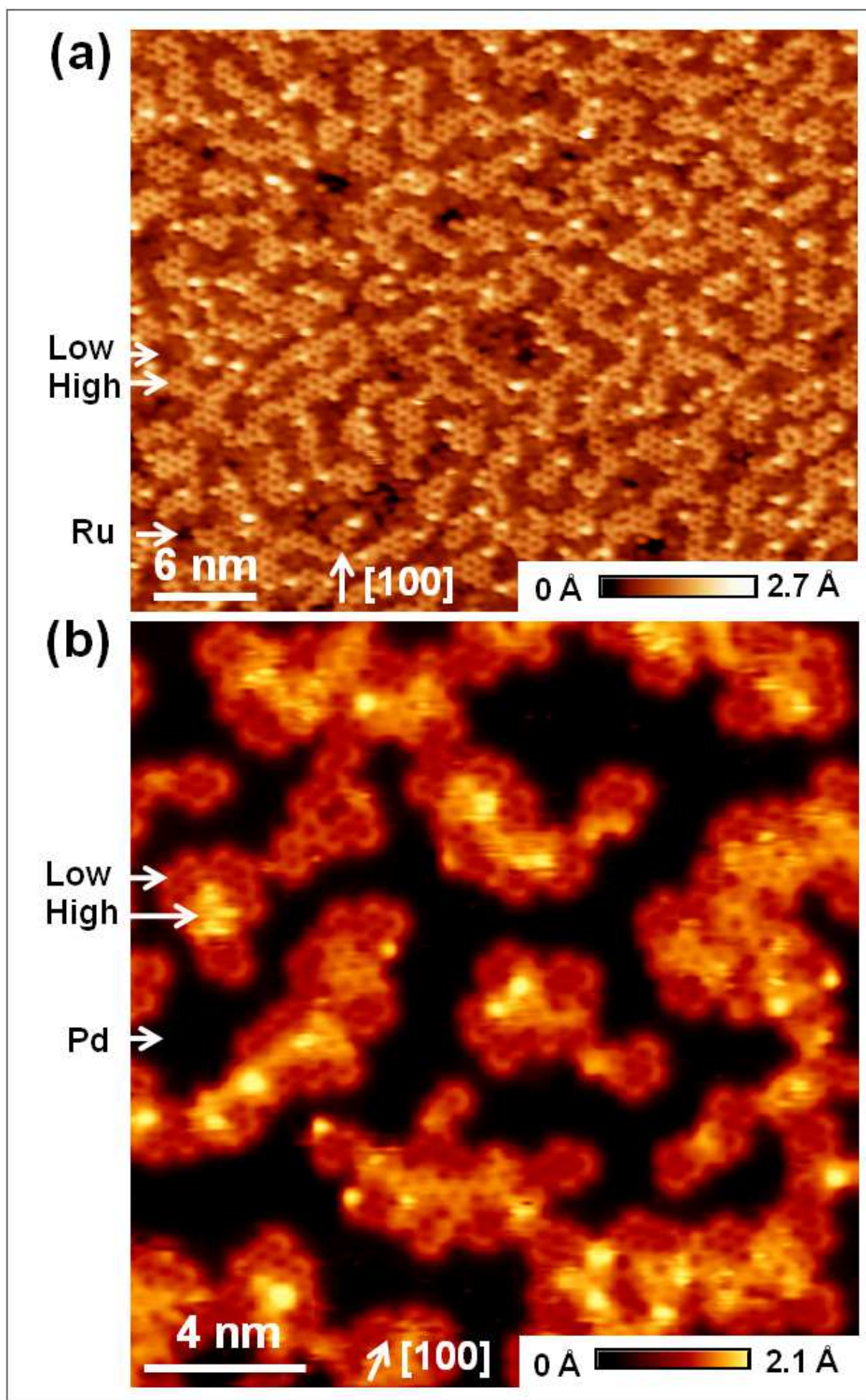


FIG. 2. (Color online) High resolution STM images of one-molecule-thick water structures formed on (a) Ru(0001) and (b) Pd(111). These structures are obtained after water adsorption at 50 K on Ru and 40 K on Pd followed by heating to 110 K on Ru and 80 K on Pd. H_2O was used on Ru(0001) and D_2O on Pd(111). The images reveal hexagonal domains with two distinct height levels, labeled with *High* and *Low*. The close-packed crystallographic directions of the substrates are indicated by the arrow at the bottom. Imaging parameters: (a) 7 K, 57 pA, -38 mV (b) 80 K, 156 pA, -124 mV.

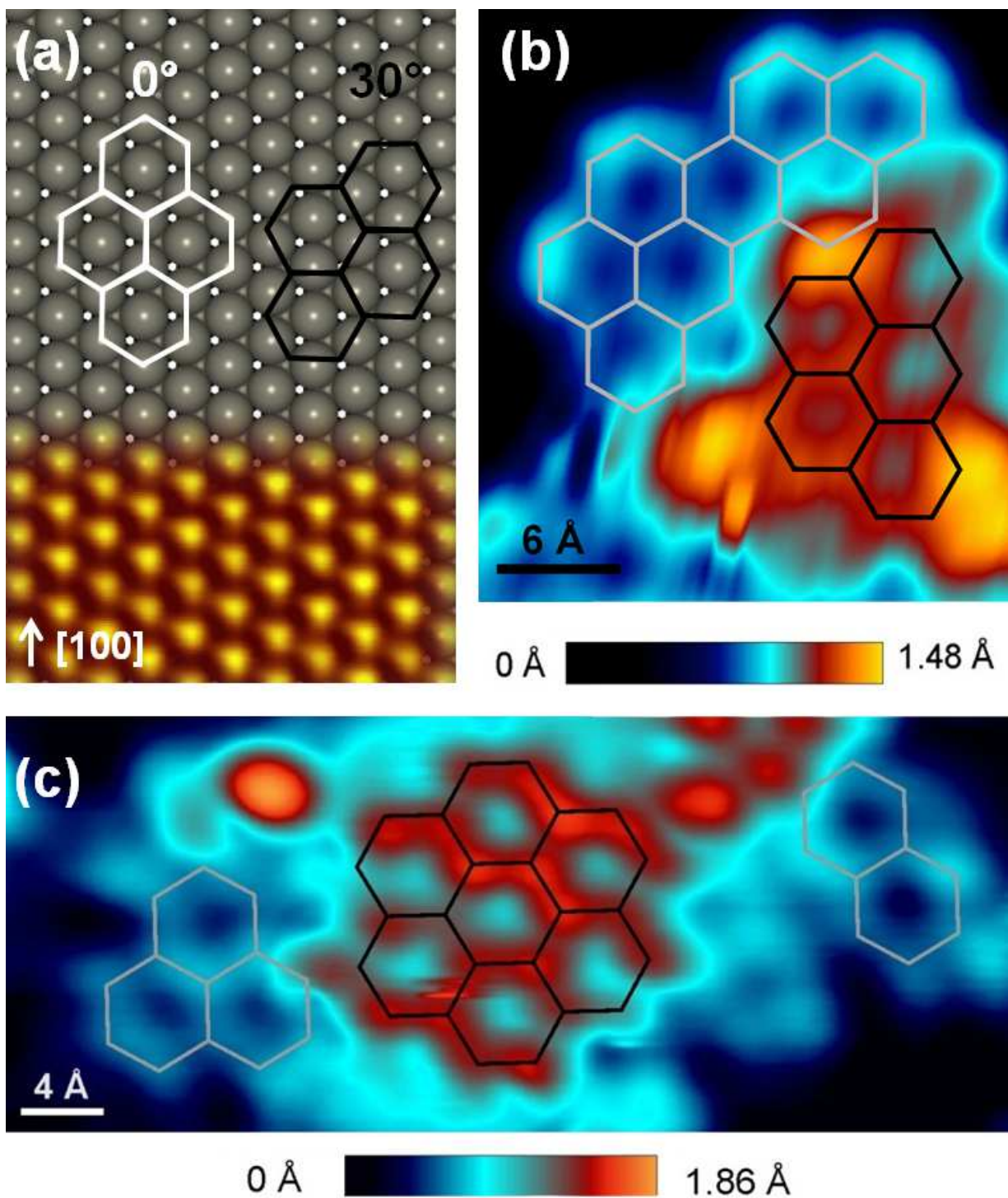


FIG. 3. (Color online) (a) Schematic illustration with clusters composed of 0° and 30° rotated hexagons on a close-packed surface. The lower part (yellow) shows an experimental atomically resolved image of Ru(0001) (Ru atoms = bright spots) before water adsorption. (b)-(c) High resolution STM images of one molecule thick (b) D_2O clusters on Pd(111) and (c) H_2O on Ru(0001) obtained after adsorption at 40 K on Pd and 50 K on Ru followed by heating to 80 K on Pd and 110 K on Ru. The images reveal hexagonal domains with two distinct height levels. The lower-lying domains (blue) are marked by gray hexagons, while the higher ones (red) are marked by black hexagons. The lower-lying hexagonal structure is in registry with the surface lattice. Unexpectedly however, the higher-lying structures are rotated by 30° . The close-packed substrate directions in the three images are the same. Imaging parameters: (b) 80 K, 156 pA, -124 mV (c) 7 K, 25 pA, -72 mV

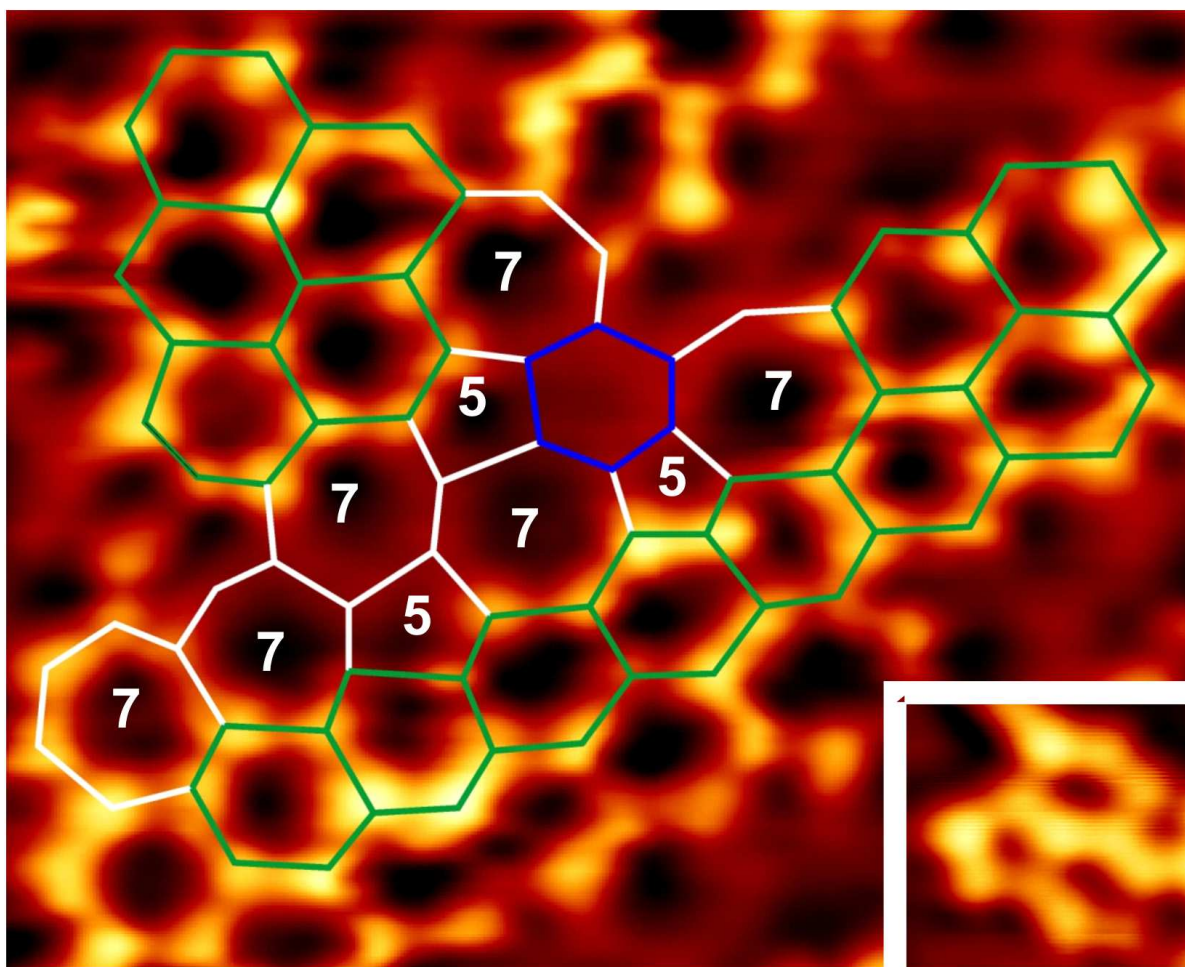


FIG. 4. (Color online) STM image (4.2 nm x 3.4 nm) showing pentagonal and heptagonal defects (marked by white lines) in the first water layer on Ru(0001), which bridge hexagonal rings in registry with the substrate (blue), and hexagonal rings rotated 30° relative to the metal lattice (green). Water was adsorbed at 140 K and subsequently imaged at 78 K. The inset shows a pentagonal ring of water molecules (H_2O adsorption at 50 K followed by heating at 110 K and imaging at 7 K). STM image parameters: 11 pA, 175 mV, inset: 86 pA, -11 mV.

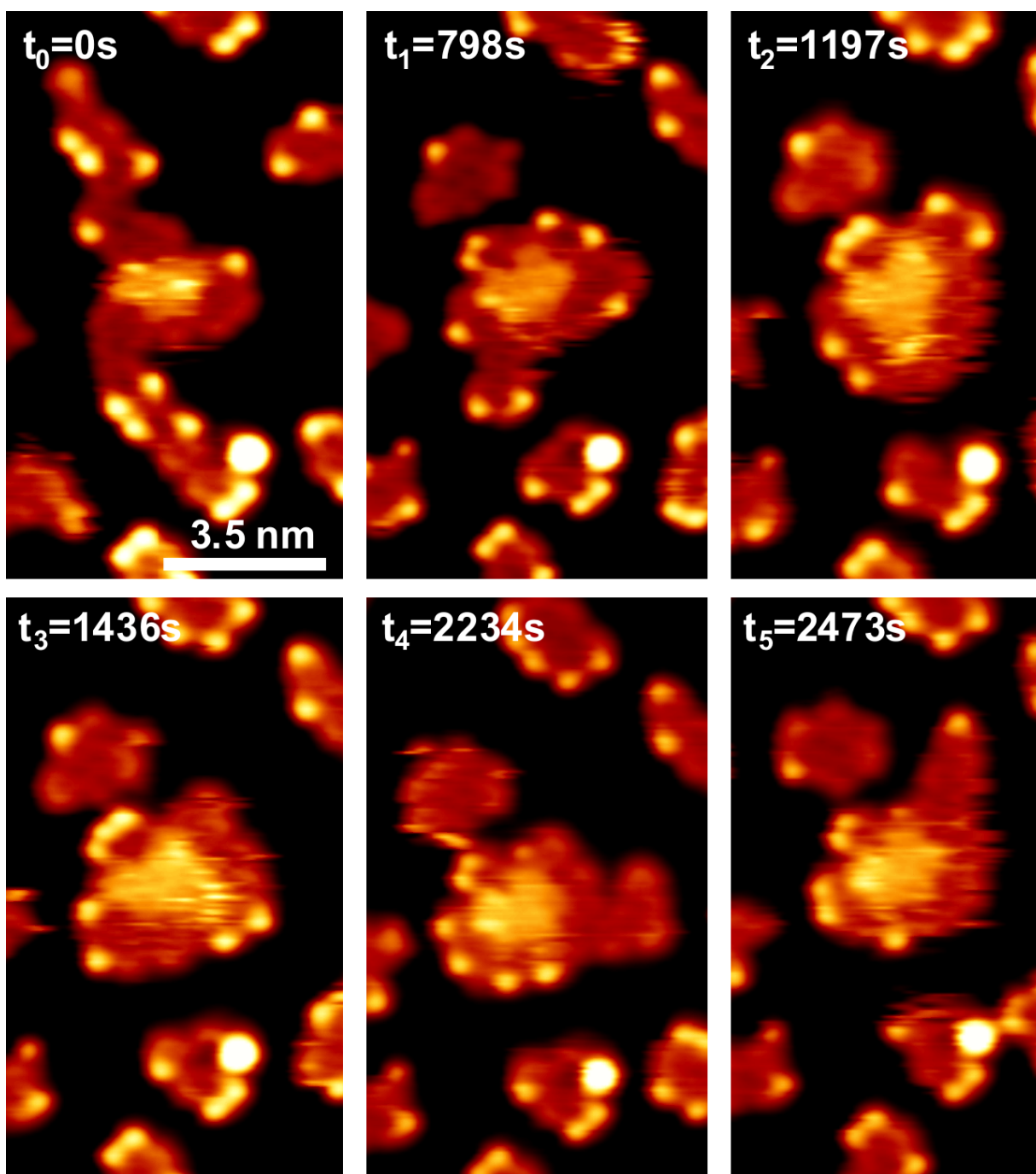


FIG. 5. (Color online) Series of topography images of D_2O clusters on Pd(111) capturing the rearrangement of water molecules on the surface. The images, recorded at a sample temperature of around 100 K, show notable rearrangement of the molecules as the size and shape of both low and high lying water domains changes from frame to frame. Note that in all images the higher-lying water molecules are located toward the center of the cluster surrounded by low lying molecules. The brighter spots on the edge of the islands (160-180 pm above the surface) correspond to molecules H-bonded to the periphery. They interact only weakly with the substrate metal atoms.¹² The time stamp in the upper left corner refers to the time passed since the first image was recorded. Water was adsorbed at 100 K and annealed approximately 1700 s at this temperature before recording the first image shown in this figure.

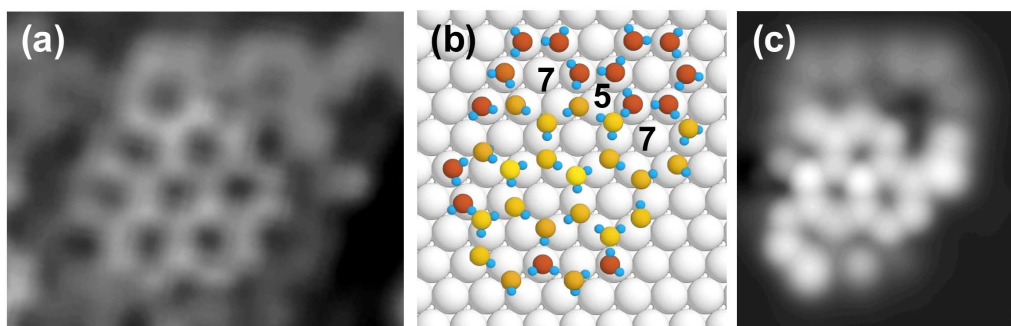


FIG. 6. (Color online) Comparison of experimental and calculated STM images of water adsorbed on Ru(0001). (a) High resolution STM image showing water hexamers rotated by 0° and 30° relative to the surface lattice and connected by pentagons and heptagons. (b) Structural model optimized by DFT calculations. The brown colored oxygen atoms are located between 2.3 and 2.5 Å above the Ru atoms in the first layer, while the height of the yellow ones is 4.4 Å, and that of the orange ones is close to 3.5 Å. (c) Calculated STM image based on the DFT optimized structure shown in (b). STM image parameters: -137 mV and 145 pA. Water was deposited at 50 K and annealed to 130 K prior imaging at 50 K.